SCIENCE CHINA
Chemistry

• ARTICLES •
SPECIAL TOPIC: Chemical Challenges in Nuclear Fuel Cycle

November 2014 Vol.57 No.11: 1483–1490
doi: 10.1007/s11426-014-5204-x

# Adsorption of thorium(IV) on magnetic multi-walled carbon nanotubes

LIU Peng[1], QI Wei[1], DU YaoFang[1], LI Zhan[2], WANG Jing[1], BI JuanJuan[1] & WU WangSuo[1,3*]

[1]*Radiochemistry Laboratory, Lanzhou University, Lanzhou 730000, China*
[2]*Institute of Modern Physics, Chinese Academy of Sciences, Lanzhou 730000, China*
[3]*State Key Laboratory of Applied Organic Chemistry, Lanzhou University, Lanzhou 730000, China*

Received May 22, 2014; accepted June 10, 2014; published online October 9 2014

The influences of pH, contact time, solid-liquid ratio, temperature and $C_{60}(C(COOH)_2)_n$ on Th(IV) adsorption onto the magnetic multi-walled carbon nanotubes (MMWCNTs) were studied by batch technique. The dynamic process showed that the adsorption of Th(IV) onto MMWCNTs could reach equilibrium in 40 h and matched the pseudo-second-order kinetics model. The adsorption of Th(IV) onto MMWCNTs was significantly dependent on pH values, the adsorption ratio increased markedly at pH 3.0–5.0, and then maintained a steady state as pH values increased. At low pH, different $C_{60}(C(COOH)_2)_n$ content could enhance the adsorption content of Th(IV) onto MMWCNTs, but restrained it at higher pH. Through simulating the adsorption isotherms by Langmuir, Freundlich and Dubini-Radushkevich models, it could be seen respectively that the adsorption pattern of Th(IV) onto MMWCNTs was mainly surface complexation, and that the adsorption process was endothermic and irreversible.

**Th(IV), adsorption, MMWCNTs, water-soluble fullerene**

## 1 Introduction

With the world energy crisis deepening, nuclear power has been vigorously developed, and thorium has attracted much attention as a potential nuclear fuel. Because the radioactive thorium can enter into the biosphere, research on the purification of thorium pollutants in water environments is important. Thorium is only stable at its valence +IV state in solution. It is usually used as a chemical analogue of tetravalent radionuclides which are difficult to study and keep in the tetravalent form [1]. In recent decades, the adsorption of Th(IV) onto different sorbents, (e.g., natural clay minerals and oxides by precipitation) as well as its surface complexation and adsorption methods have been extensively studied. Guo *et al*. [2], who studied the adsorption of Th(IV) onto $TiO_2$ at different pH values, indicated that the adsorption behavior was strongly influenced by the pH changes and that the adsorption quantity obviously increased in the presence of phosphate in aqueous solution. Wu *et al.* [3] studied the adsorption process of Th(IV) onto attapulgite, which was also influenced by changes in pH, and found the adsorption process of Th(IV) onto attapulgite was a spontaneous process. In addition, the sorption-desorption hysteresis indicated that the sorption of Th(IV) was irreversible. Chen *et al.* [4] studied the adsorption of Th(IV) onto silica with the presence of humic/fulvic acid; in their work, the adsorption process was significantly dependent on pH, temperature and humic/fulvic acid content.

Carbon nanotubes (CNTs), a kind of carbon allotrope with typical layered hollow structure, are considered to be a typical one-dimensional (1D) material. The strong adsorptive

*Corresponding author (email: wuws@lzu.edu.cn)

interaction between carbon nanotubes and radionuclides or organic aromatic pollutants is attributed to π-π electron-donor acceptor interaction between the pollutants and the highly polarizable carbon nanotubes; therefore the strong surface complexation between metal ions and functional groups is considered to be the main mechanism of metal ions adsorption onto carbon nanotubes [5–7]. Due to their special structure, carbon nanotubes have large specific surface area and high chemical stability. In addition the surface modification of MWCNTs to graft functional groups can improve the adsorption capacity of MWCNTs in the removal of most radionuclides and organic pollutants from large volumes of aqueous solutions [8]. Therefore, carbon nanotubes have excellent physiochemical properties and versatile applications, especially in the fileds of mechanics, electromagnetism, optics, electronics, catalysis, and composite materials, and have huge potential research value [9, 10]. Some researchers have done many studies about metal ions (specifically, adsorption of Pb(II), Ni(II), Cd(II)) onto oMWCNTs) [11–13]. Sun *et al*. [7] studied the adsorption behavior of diuron, fluridone, and norflurazon on single-walled and multi-walled carbon nanotubes; their results indicated that MWCNTs had the potential to serve as an adsorbentto reduce the mobility of herbicides in agricultural and environmental applications. Wang *et al*. [14] studied the adsorption of humic acid to functionalized multi-walled carbon nanotubes and indicated that the adsorption process was dependent on the nanotubes' surface area and meso- and macro-pore volumes.

CNTs suffer from separation inconvenience, however. In order to improve their properties and functions with the aim of extending their applications in various technology fields, their surface are coated with iron oxide nanoparticles [15]. Due to their unique structures, CNT composites have great potential as superior adsorbents for removing many contaminants. Compared with experimental environments, the natural environment is more complicated [16]. Because few studies have been done on the behavior of other organic materials in the adsorption of metal ions in the presence of carbon nanomaterials, it's important to study the effects of a variety of carbon nanomaterials on the adsorption of metal ions. The least expensive and most easilyobtained material, $C_{60}$, easily forms π-π stacking with other aromatic materials because of their large numbers of π electrons [17, 18], For these reasons, $C_{60}$ has been used to investigate these materials' adsorption properties through improving solubility by adding the appropriate functional groups to the fullerence skeleton [19]. In our work, water-soluble fullerene derivatives were selected as additional factors with in the ternary system in order to study the adsorption of metal ions and to simulate the interactions of carbon nanomaterials with metal ions in real environmental conditions. Our intention was through which to provide a theoretical basis for radioactive thorium purification issues.

## 2 Materials and methods

### 2.1 Materials

Multi-wall carbon nanotubes (L. MWNTs-1030) materials, purity > 95% (amorphous carbon ⩽ 3 wt%, ash content ⩽ 0.2 wt%), diameter 10–30 nm, length 5–15 μm, specific surface area 10–100 $m^2$/g, were purchased from Shenzhen Nanotech Port Company (Shenzhen, China). $FeCl_2{\cdot}H_2O$ and $FeCl_2{\cdot}H_2O$ with a molar ratio of l:2 were mixed in deionized water. Next, 10 mL of 2 mol/L HCl was added. The solution was heated to 30 °C under nitrogen protection and then stirred at 30 °C at a constant pH value of 9 for 1 h. The precipitates were continuously mixed under constant heating at 50 °C for 30 min. After being cooled to room temperature, the obtained magnetic nanoparticles were washed with water and ethanol several times and then dried under vacuum at 60 °C overnight. The typical procedure for the preparation of $Fe_3O_4$/MWCNT composite was as follows: 3 g MWCNTs was dispersed into 150 mL of concentrated $HNO_3$, followed by bath heating at 110 °C for 5 h. The solution was diluted with deionized water until the pH value of the filtrate almost reached 7. After being rinsed and dried, 200 mg acid-purified nanotubes and 50 mg $Fe_30_4$ nanoparticles were dispersed in 40 mL solution of deionized water/ethanol (volume ratio = 1:1). The mixture was ultrasonicated for 1 h and then stirred at room temperature for 96 h. The solution was separated from the residue through 200 μm filter membrane, followed by vacuum drying at 50 °C for 16 h [20].

Fullerene ($C_{60}$), purity > 99.9%, was purchased from the Yongxin Technology Co. Ltd. (Puyang, China). The $C_{60}$ and NaH were added into toluene; when the color of the mixture solution changed from purple to deep red, diethyl bromomalonate was added. The solution was stirred at 80 °C under the protection of Ar gas for 10 h and then concentrated by rotary evaporator. Next, the residue was dissolved in the toluene and NaH was added. Then, $CH_3OH$ was added to the solution to immediately terminate the reaction, followed by 2 mol/L HCl. The precipitate was filtred, collected, and washed by toluene, 2 mol/L HCl, $H_2O$, and benzene [21].

Unless otherwise noted, materials were obtained from commercial suppliers and were used without further purication.

### 2.2 Batch experiments

Adsorption experiment: after determining the equilibrium time and the solid-liquid ratio, a series of polyethylene centrifuge tube were added a certain amount of MMWCNTs, $NaNO_3$ and a known concentration Th(IV) solution, such that the various components of the system achieved the required concentration. The extremely small amounts of HCl or NaOH solution were added to the system to adjust its pH to a desired value. The system was centrifuged at high-

speed (12000 r/min) for 20 min after constant temperature oscillation for 72 h. A certain volume of supernatant was removed to detect the concentration of Th(IV) by using spectrophotometer (Perkin-Elmer, USA) at a wavelength of 664 nm. The adsorption of Th(IV) onto the MMWCNTs was calculated from the difference between the concentrations initially concentration and at equilibrium.

Desorption experiment: the same solution was created as in the adsorption experiment above. A certain volume of supernatant was removed after the solution was centrifuged. The same volume of $NaNO_3$ was added to the rest of the solution, and the pH was adjusted. About after 6 d, the sample was centrifuged and measured.

### 2.3 Transmission electron microscopy (TEM) analysis

In order to analyze the molecular level information of the adsorbent material, transmission electron microscopy (TEM, Hitachi Model H-600, Japan) was conducted (Figure 1). Figure 1 shows the tiny nanoparticles consist of $Fe_3O_4$ with a diameter of 10–30 nm, were well attached to the CNTs. Figure 2 shows that magnetic separation process in which the magnetic composites were moved from aqueous solutions with a permanent magnet. Figure 2(a) shows the unseparated MMWCNTs: the solutions are quite muddy. Conversely, Figure 2(b) shows that the solution was very clear, which means that the magnetic composites could be easily separated from the aqueous solution. This magnetic separation method can be applied simply and widely in real work.

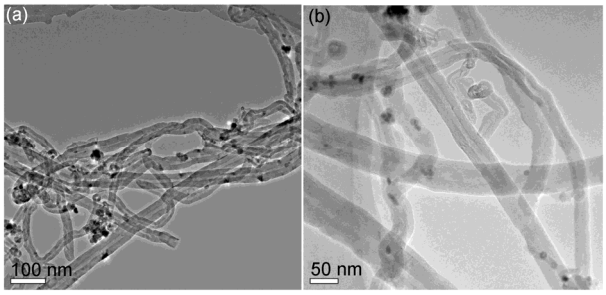


**Figure 1** The TEM of magnetic nanomaterials. (a) MWCNTs; (b) MMWCNT.

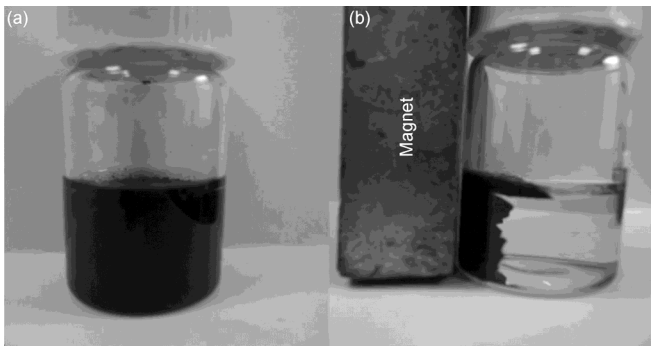


**Figure 2** Separation of the magnetic composites in the presence of a permanent magnet.

## 3 Results and discussion

### 3.1 Adsorption kinetics

*Effect of contact time on the adsorption of Th(IV) onto MMWCNTs*

The influence of the duration of shaking time on the adsorption of Th(IV) onto MMWCNTs is shown in Figure 3. The adsorption ratio increased with the increasing of time; however, after the contact time (about 40 h) was reached, the adsorption ratio was substantially unchanged. The initial adsorption rate was higher, which might be attributed to the great quantity of adsorption sites on the surface of magnetic composites. As the sites were gradually occupied by Th(IV), the adsorption rate became slower. Figure 3 shows that the chemical adsorption or surface complexation was the main sorption mechanism, rather than physical adsorption [12]. In the following experiments, 72 h was selected as the equilibrium time.

*Pseudo-second-order equation*

The pseudo-second-order kinetic equation linear expression is as follows:

$$\frac{t}{q_t} = \frac{1}{kq_e^2} + \frac{t}{q_e} \quad (1)$$

where $q_e$ (mg/g) is the equilibrium adsorption amount and $q_t$ is the adsorption amount of dye at time $t$. The parameter $k$ (g/(mg min)) represents the second-order rate constant of the kinetic model. The results of using this equation to fit the experimental data are shown in Figure 4. The pseudo-second-order equation was $y = 146.3x + 59.9$; calculated by the slope and intercept of $k = 361.01$ g/(mg min), the $q_e = 0.0068$ mg/g, and the linear correlation coefficient $R^2 = 0.9999$. These results show that the adsorption of Th(IV) onto MMWCNTs was in keeping with the pseudo-second-order kinetic model.

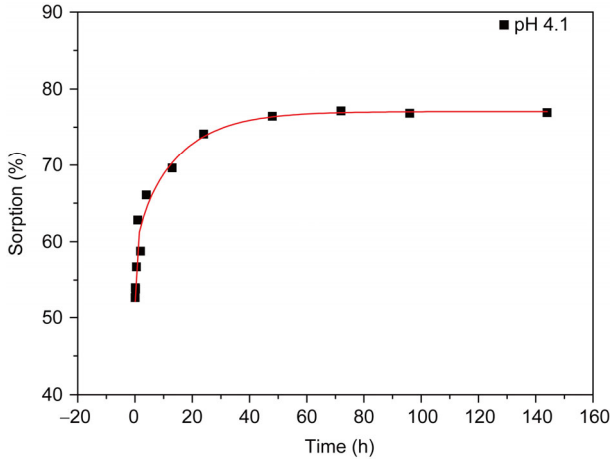


**Figure 3** Effect of equilibrium time on Th(IV) adsorption onto MMWCNTs. pH 4.10 ± 0.05, $m/V = 0.10$ g/L, $T = (25 \pm 1)$ °C, $C_{Th}^0 = 7.09 \times 10^{-5}$ mol/L.

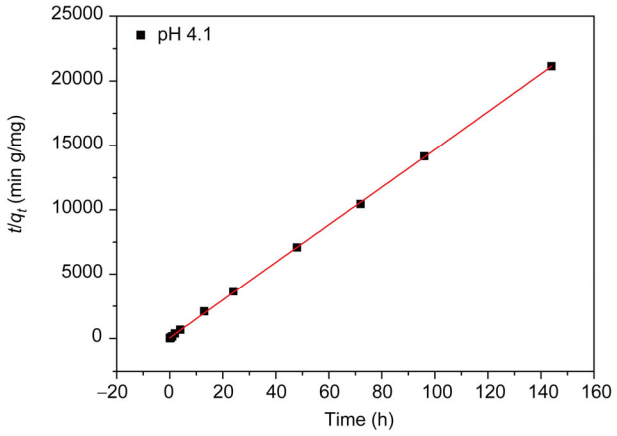


**Figure 4** Pseudo-second-order sorption kinetics plot for Th(IV). pH 4.10 ± 0.05, $m/V$ = 0.10 g/L, $T$ = (25 ± 1) °C, $C_{Th}^0$ = 7.09 × $10^{-5}$ mol/L.

### 3.2 Effect of pH on Th(IV) adsorption onto MMWCNTs

We studied the adsorption of Th(IV) as a function of pH under different background electolytes, such as 0.001, 0.01, 0.05, and 0.1 mol/L $NaNO_3$ solutions. The influence of different pH on the adsorption are shown in Figure 5, the adsorption ratio of Th(IV) onto MMWCNTs was strongly influenced by pH and ionic strength. Sheng *et al.* [22] found that the adsorption ratio of Th(IV) on raw diatomite increased rapidly to almost 100% when the pH value changed from 2 to 4; in addition, the adsorption ratio was influenced by the ionic strength. Our results showed that the adsorption rate increased as the concentration of $NaNO_3$ increased (Figure 5); Qian *et al*. [23] and Wang *et al*. [24] found that the adsorption of Th(IV) on zirconium oxo-phosphate and oxidized multi-walled carbon nanotubes was effected both by ionic strength and pH changes. The experimental results of this work further confirmed the previous results.

When pH < 3.0, the adsorption ratio was low and changed hardly at all as the pH increased. In the range of pH 3.0 to 5.0, the adsorption ratio increased rapidly. When pH > 5.0, the adsorption ratio changed inconspicuously, which indicated that the system was in equilibrium.

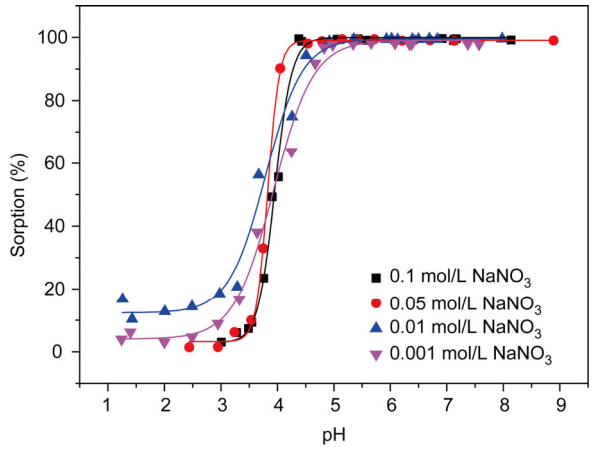


**Figure 5** Effect of pH on Th(IV) adsorption onto MMWCNTs. $m/V$ = 0.10 g/L, $T$ = (25±1) °C, $C_{Th}^0$ = 7.09 × $10^{-5}$ mol/L.

It was necessary to inspect the speciation of Th(IV) in solution with different pH to discuss the possible species of Th(IV) in the systems. Calculations were performed for 0.01 mol/L $NaNO_3$ solutions containing 7.09 × $10^{-5}$ mol/L of total aqueous Th(IV) with pH varying from 1.0 to 10. As shown in Figure 6, the main forms were $Th^{4+}$, $Th(OH)^{3+}$, $Th(NO_3)^{3+}$, $Th(OH)_2^{2+}$, $Th(CO_3)_5^{6-}$ and $Th(OH)_3CO_3^-$. When pH ⩽ 3.0, the main species was $Th^{4+}$ at pH 3.0–5.0; the $Th(OH)_2^{2+}$ in the system accounted for its absolute dominance. However, at pH > 5.0, the two species $Th(CO_3)_5^{6-}$ and $Th(OH)_3CO_3^-$ existed in the absence of $CO_2$ because their low solubility in aqueous solution lead to an increase of the content of Th(IV) in the solid phase; therefore, the adsorption ratio of Th(IV) onto MMWCNTs maintained the maximum and no longer changed. In our previous works, we have shown that the point of zero charge was about 5 [5]; the surface charge of MMWCNTs was positive at pH < $pH_{zpc}$; and that the electrostatic repulsion between $Th^{4+}$, $Th(NO_3)^{3+}$, and the positive surface of adsorbents was strong, which caused the electrostatic repulsion for the adsorption of $Th^{4+}$ on MMWCNTs. With the increase of pH, the negative charge of the site increased as well; therefore it was reasonable that Th(IV) sorption significantly increased. At pH > $pH_{zpc}$, the mechanism was the same as pH < $pH_{zpc}$. Becausethe interaction between $Th(OH)_3CO_3^-$ and MMWCNTs was also an electrostatic interaction the effects of ionic strength were almost negligible (Figure 5).

### 3.3 Effect of solid-liquid ratio on the adsorption of Th(IV) onto MMWCNTs

Figure 7 showes that the adsorption ratio of Th(IV) onto MMWCNTs increased with the increase of MMWCNTs concentration. As the concentration of MMWCNTs increased, the surface adsorption sites also increased, which

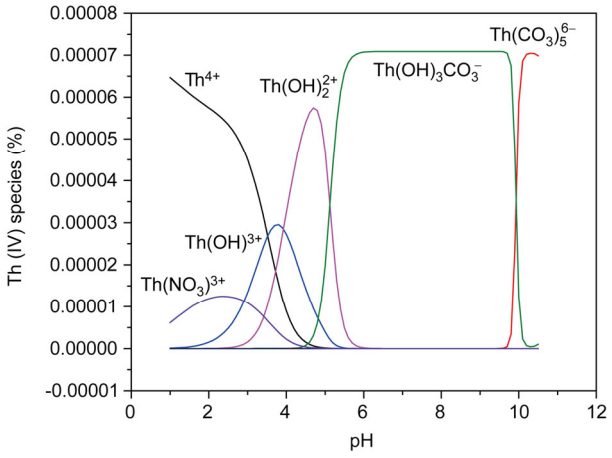


**Figure 6** Relative species distribution of Th(IV). $T$ = (25 ± 1) °C, $C_{Th}^0$ = 7.09 × $10^{-5}$ mol/L, $P_{CO_2}$ = $10^{-3.26}$ atm.

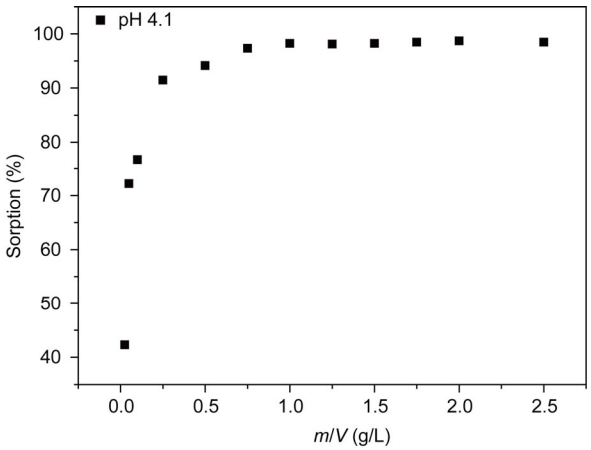


**Figure 7** Effect of solid-to-liquid ratio ($m/V$) of Th(IV) adsorption onto MMWCNTs. pH 4.10 ± 0.05, $T$ = (25 ± 1) °C, $C_{Th}^{0}$ = 7.09 × $10^{-5}$ mol/L.

promoted the adsorption of Th(IV). This phenomenon is also present in other adsorption systems [25, 26].

### 3.4 Effect of temperature on the adsorption of Th(IV) onto MMWCNTs

The influence of different temperature on the adsorption is shown in Figure 8. The thorium concentrations of solid phase ($C_s$ (mol/g)) increase with the increase of Th(IV) in solution ($C_e$ (mol/L)), and the adsorption isotherms of Th(IV) in 323 K were much higher than for Th(IV) in 298 K. This means that the adsorption of Th(IV) on MMWCNTs was endothermic.

It was necessary to propose a suitable model to gain a better understanding of the mechanism. To optimize the adsorption of Th(IV) from aqueous solutions, the Freundlich, Langmuir and D-R sorption isotherms were applied to calculate the relative adsorption data [27]. The results of experiments at different temperatures are shown in Figure 9. The three models were used most commonly used by other

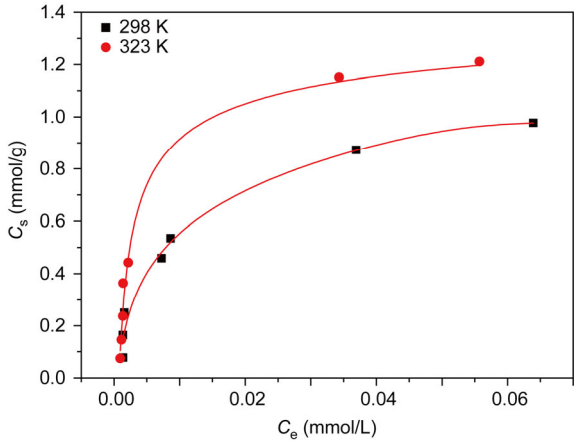


**Figure 8** Effect of different temperature on the adsorption of Th(IV) onto MMWCNTs. pH 4.10 ± 0.05, $m/V$ = 0.10 g/L, $C_{Th}^{0}$ = 7.09 × $10^{-5}$ mol/L.

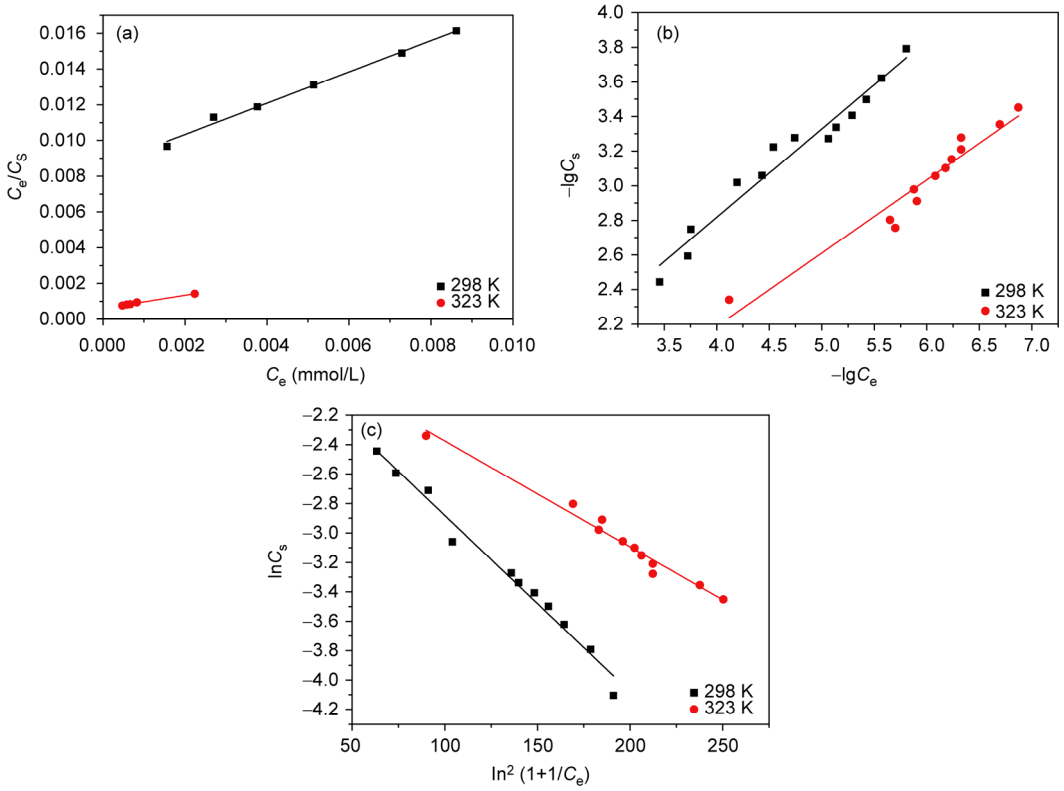


**Figure 9** The sorption isotherms of Th(IV) onto MMWCNTs. (a) Langmuir isotherm; (b) Freundlich isotherm; (c) D-R isotherm.

researchers to describe the adsorption characteristics of adsorbent in water and wastewater treatment, and the relative parameters calculated from Eqs. (2–6) are listed in Table 1. It is well known that the Langmuir model was one of the most widely used models for modeling equilibrium data and that the isotherm was valid for monolayer adsorption onto a surface that containing a finite number of identical sites [27]. This process could be described by the following form [28]:

$$\frac{C_e}{C_s} = \frac{1 + C_s \cdot K_a}{K_a \cdot q_{max}} \quad (2)$$

where $q_{max}$ (mg/g) is the capacity of adsorption at saturation and $K_a$ (L/mmol) shows the adsorption coefficient that is related to the energy of adsorption. The Langmuir isotherm could be expressed as:

$$K_a = \frac{1}{R_L \cdot C_0} - \frac{1}{C_0} \quad (3)$$

where $C_0$ (mol/L) is the concentration of initial metal in the solution. The value of $R_L$ indicates a good sorbent for the sorbate if it is between 0 and 1. The Freundlich expression is an empirical equationthat describs adsorption onto the heterogeneous surface [29]. The Freundlich isotherm model stipulates that the ratio of solute adsorbed to the solute concentration is a function of the solution. The Freundlich model also allows for several different kinds of adsorption sites on the solid, and represents the adsorption data at low intermediate concentrations on the heterogeneous surfaces [27]. The linear equation could be presented as:

$$n \ln(C_s) = n \ln K_F + \ln C_e \quad (4)$$

where $K_F$ (mmol/g) is the adsorption capacity. When the value of $n$ at 1 and 10 indicates a favorable adsorption. Because the D-R isotherm neither assume a homogeneous surface nor constant adsorption potential, it is more ordinary than the Langmuir isotherm. And the linear form of D-R equation is [27, 30]:

$$\ln q_m = \ln C_s + KR^2T^2 \ln^2\left(\frac{1 + C_e}{C_e}\right) \quad (5)$$

where $K$ shows the constant that is related to the adsorption energy, $q_m$ (mol/g) shows the theoretical saturation capacity; $R$ (kJ/(mol K)) shows the gas constant and $T$ (K) is the temperature. The free energy of adsorption $E$ (kJ/mol) is defined as when one molecule of ion is transferred from infinity in solution to the surface of the solid and the free energy changed. It could be calculated from the value of $K$ using the following equation [27]:

$$E = \sqrt{\frac{1}{2K}} \quad (6)$$

The magnitude of $E$ is widely used for estimating the type of adsorption reaction. If the value of $E$ is between 8–16 kJ/mol, the adsorption must be governed by chemical ion-exchange; if $E > 16$ kJ/mol, it could be supposed that particle diffusion may affect the adsorption [27]. The adsorption may be effected by physical forces if $E < 8$ kJ/mol [27, 31].

**Table 1** Comparison of the Langmuir, Freundlich and D-R adsorption constants of Th(IV) onto MMWCNTs

| Isothermal model parameters | 298 K | 323 K |
|---|---|---|
| Langmuir | | |
| $K_a$ (L/mmol) | $1.019 \times 10^{-5}$ | $6.011 \times 10^{-5}$ |
| $q_{max}$ (mmol/g) | 0.001 | 0.003 |
| $R_L$ | 0.122 | 0.023 |
| $R^2$ | 0.991 | 0.993 |
| Freundlich | | |
| $K_F$ (mmol/g) | 2.168 | 1.639 |
| $n$ | 1.961 | 2.364 |
| $R^2$ | 0.957 | 0.931 |
| D-R | | |
| $K$ (mol$^2$/kg$^2$) | $1.900\times10^{-9}$ | $1.200\times10^{-9}$ |
| $q_m$ (mol/g) | 0.186 | 0.191 |
| $E$ (kJ/mol) | 16222.142 | 20412.415 |
| $R^2$ | 0.980 | 0.973 |

It could be concluded from the constants that the Langmuir and D-R models fitted the experimental data better than the Freundlich model did. In all cases, the Freundlich isotherm represented the poorest fit of experimental data as indicated by $R^2$ values. The fact that the Langmuir isotherm fit the experimental data very well indicated almost complete monolayer coverage of the adsorbent particles. The adsorption capacities $q_m$ derived in the D-R model for the adsorption of Th(IV) was 0.186 mol/g at 298 K, and 0.191 mol/g at 323 K. These values were quite different from the adsorption capacity $q_{max}$ values at the Langmuir region. This difference, which has been reported in other works [27, 32, 33]. might be attributed to the different assumptions considered in the formulation of the isotherms.

### 3.5 Effect of $C_{60}(C(COOH)_2)_n$ on the adsorption of Th(IV) onto MMWCNTs

The effect of $C_{60}(C(COOH)_2)_n$ on the adsorption of Th(IV) is shown in Figure 10. At the initial state of the adsorption, $C_{60}(C(COOH)_2)_n$ enhanced the adsorption, but the adsorption was restrained at higher pH. As is well known, there are many benzene ring structures of $C_{60}(C(COOH)_2)_n$ that can form a strong π-π interaction with MMWCNTs. The previous discussion showed that the adsorption process of Th(IV) onto MMWCNTs was mainly surface complexation (Figure 3). $C_{60}(C(COOH)_2)_n$ also had some macromolecular structures that could interact with Th(IV) through surface complexation or chemical adsorption. It is reported that the π-π interaction is stronger than that of surface complexation [5]. Therefore, in this experiment, at the same concentration of MMWCNTs system (or at the same adsorption sites), the Th(IV) was adsorbed onto MMWCNTs through surface complexation until to get maximum adsorption ration in the

absence of $C_{60}(C(COOH)_2)_n$ (about 100%, Figure 10). When the $C_{60}(C(COOH)_2)_n$ presented in the adsorption system, it occupied the sites of MMWCNTs first through π-π interaction. $C_{60}(C(COOH)_2)_n$ could also interact with Th(IV) by surface complexation or chemical adsorption, however, because its macromolecular structures were smaller than those of MMWCNTs. In other words, the specific surface area of $C_{60}(C(COOH)_2)_n$ was larger than that of the MMWCNTs, meaning that the interaction ability of Th(IV) with $C_{60}(C(COOH)_2)_n$ was stronger than with MMWCNTs Therefore, the presence of $C_{60}(C(COOH)_2)_n$ could improve the adsorption rate of Th(IV) onto MMWCNTs depending on the concentration of $C_{60}(C(COOH)_2)_n$, but it would not affectthe maximum adsorption rate (Figure 10). However, when the pH of the solution was higher than 6, the Th(IV) adsorbed by the $C_{60}(C(COOH)_2)_n$ and MMWCNTs could desorb into solution (Figure 10). This result might be attributed to the species changes of Th(IV) in different pH solutions, which preventedthe interaction of Th(IV) with $C_{60}(C(COOH)_2)_n$. The sites of the MMWCNTs were also occupied by $C_{60}(C(COOH)_2)_n$, however, which means that the adsorption ratio of Th(IV) onto MMWCNTs decreased with the increase of pH in solution.

The effect of $C_{60}(C(COOH)_2)_n$ concentration on the adsorption ratio when the ratio of solid to liquid is at pH 4.10 ± 0.05 are shown in Figure 11. The adsorption ratio increased with the increase of the *m*/*V* untill the adsorption process reached the maximum value at the experimental conditions, which might be attributed to the increase of surface adsorption sites. It might also be possible that the $C_{60}(C(COOH)_2)_n$ was was favorable to the adsorption.

### 3.6 Adsorption and desorption isotherms

Figure 12 shows that, whether or not $C_{60}(C(COOH)_2)_n$ was present, the desorption isotherm was obviously higher than the adsorption isotherm. This result indicates that Th(IV) adsorbed onto solid particles could not be desorbed from solid to liquid phase to reestablish equilibrium under the experimental conditions. Instead, the adsorption-desorption hysteresis actually occurred and the adsorption process was irreversible. These results indicate that strong surface

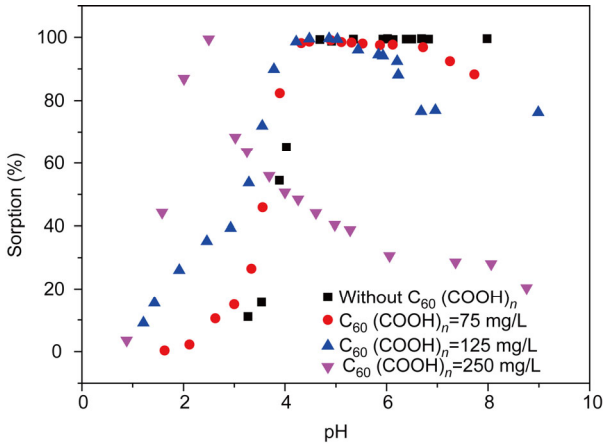


**Figure 10** Effect of $C_{60}(C(COOH)_2)_2$ on the adsorption of Th(IV) onto MMWCNTs. pH 4.10 ± 0.05, $m/V$ = 0.10 g/L, $T$ = (25 ± 1) °C, $C_{Th}^0$ = 7.09 × $10^{-5}$ mol/L.

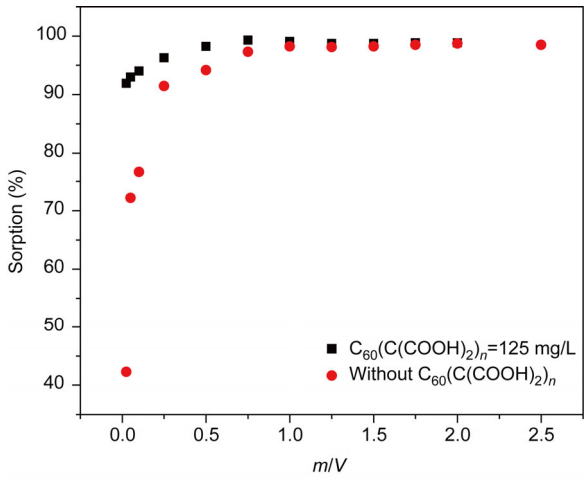


**Figure 11** Effect of solid to liquid ratio (g/L) and $C_{60}(C(COOH)_2)_n$ concentrations on the adsorption of Th(IV) onto MMWCNTs. pH 4.10 ± 0.05, $T$ = (25 ± 1) °C, $C_{Th}^0$ = 7.09 × $10^{-5}$ mol/L.

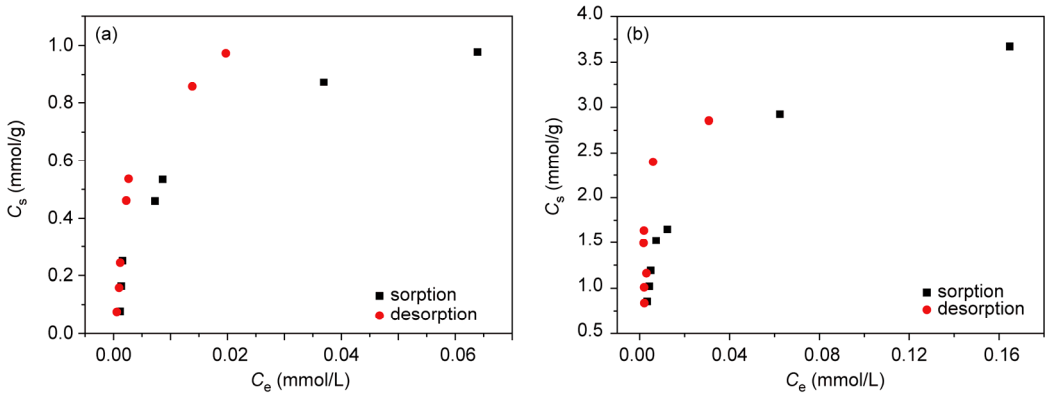


**Figure 12** Sorption and desorption isotherms of Th(IV) onto MMWCNTs (a) and in the present of $C_{60}(C(COOH)_2)_n$ (b).

complexes were produced at the surface of MMWCNTs by chemical sorption rather than physical sorption. Similar experimental results were also reported by previous researchers [3, 27, 34–36].

## 4 Conclusions

The effects and behavior of Th(IV) adsorption onto MMWCNTs were studied in the presence of $C_{60}(C(COOH)_2)_n$. The adsorption and desorption isotherms shows that the adsorption of Th(IV) on MMWCNTs was endothermic and irreversible. The adsorption of Th(IV) onto MMWCNTs was affected strongly by pH, and the presence of $C_{60}(C(COOH)_2)_n$ obviously influenced the adsorption ratio. Therefore, for the appropriate adsorption system of Th(IV) in practical work, some macromolecular structures with π-π interactions may improve the adsorption effect.

*This work was financially supported by the National Natural Science Foundation of China (J1210001).*


1 Xu D, Chen CL, Tan XL, Hu J, Wang XK. Sorption of Th(IV) on Na-rectorite: effect of HA, ionic strength, foreign ions and temperature. *Appl Geochem*, 2007, 22: 2892–2906
2 Guo ZJ, Niu LJ, Tao ZY. Sorption of Th(IV) ions onto $TiO_2$: effects of contact time, ionic strength, thorium concentration and phosphate. *J Radioanal Nucl Chem*, 2005, 266: 333–338
3 Wu WS, Fan QH, Xu JZ, Niu ZW, Lu SS. Sorption-desorption of Th(IV) on attapulgite: effects of pH, ionic strength and temperature. *Appl Radiat Isot*, 2007, 65: 1108–1114
4 Chen C, Wang X. Sorption of Th (IV) to silica as a function of pH, humic/fulvic acid, ionic strength, electrolyte type. *Appl Radiat Isot*, 2007, 65: 155–163
5 Wang J, Li Z, Li SC, Qi W, Liu P, Liu YL, Ye YL, Wu LS, Wang L, Wu WS. Adsorption of Cu (II) on oxidized multi-walled carbon nanotubes in the presence of hydroxylated and carboxylated fullerenes. *PloS One*, 2013, 8: e72475
6 Tang WW, Zeng GM, Gong JL, Liu Y, Wang XY, Liu YY, Liu ZF, Chen L, Zhang XR, Tu DZ. Simultaneous adsorption of atrazine and Cu(II) from wastewater by magnetic multi-walled carbon nanotube. *Chem Eng J*, 2012, 221: 470–478
7 Sun K, Zhang ZY, Gao B, Wang ZY, Xu DY, Jin J, Liu XT. Adsorption of diuron, fluridone and norflurazon on single-walled and multi-walled carbon nanotubes. *Sci Total Environ*, 2012, 439: 1–7
8 Abbaspour A, Izadyar A. Carbon nanotube composite coated platinum electrode for detection of Cr(III) in real samples. *Talanta*, 2007, 71: 887–892
9 Heath JR. Nanoscale materials. *Accounts Chem Res*, 1999, 32: 388
10 Schierz A, Zänker H. Aqueous suspensions of carbon nanotubes: surface oxidation, colloidal stability and uranium sorption. *Environ Pollut*, 2009, 157: 1088–1094
11 Xu D, Tan XL, Chen CL, Wang XK. Removal of Pb (II) from aqueous solution by oxidized multiwalled carbon nanotubes. *J Hazard Mater*, 2008, 154: 407–416
12 Yang ST, Li JX, Shao DD, Hu J, Wang XK. Adsorption of Ni (II) on oxidized multi-walled carbon nanotubes: effect of contact time, pH, foreign ions and PAA. *J Hazard Mater*, 2009, 166: 109–116
13 Tian XL, Li TT, Yang K, Xu Y, Lu HF, Lin DH. Effect of humic acids on physicochemical property and Cd(II) sorption of multiwalled carbon nanotubes. *Chemosphere*, 2012, 89: 1316–1322
14 Wang F, Yao J, Chen HL, Yi ZJ, Xing BS. Sorption of humic acid to functionalized multi-walled carbon nanotubes. *Environ Pollut*, 2013, 180: 1–6
15 Lu SS, Chen L, Dong YH, Chen YX. Adsorption of Eu (III) on iron oxide/multiwalled carbon nanotube magnetic composites. *J Radioanal Nucl Chem*, 2011, 288: 587–593
16 Hyung H, Kim JH. Natural organic matter (NOM) adsorption to multi-walled carbon nanotubes: effect of NOM characteristics and water quality parameters. *Environ Sci Technol*, 2008, 42: 4416–4421
17 Bühl M, Hirsch A. Spherical aromaticity of fullerenes. *Chem Rev*, 2001, 101: 1153–1183
18 Montes-Moran M, Suárez D, Menéndez JA, Fuente E. On the nature of basic sites on carbon surfaces: an overview. *Carbon*, 2004, 42: 1219–1225
19 Troshin PA, Hoppe H, Renz J, Egginger M, Mayorova JY, Goryachev AE, Peregudov AS, Lyubovskaya RN, Gobsch G, Serdar Sariciftci N, Razumov VF. Material solubility-photovoltaic performance relationship in the design of novel fullerene derivatives for bulk heterojunction solar cells. *Adv Funct Mater*, 2009, 19: 779–788
20 Fan XJ, Li X, Preparation and magnetic property of multiwalled carbon nanotubes decorated by $Fe_3O_4$ nanoparticles. *New Carbon Mater*, 2012, 27: 111–116
21 Cheng FY, Yang XL, Zhu HS, Sun J, Liu Y. Synthesis of oligoadducts of malonic acid $C_{60}$ and their scavenging effects on hydroxyl radical. *J Phys Chem Solids*, 2000, 61: 1145–1148
22 Sheng G, Hu J, Wang X. Sorption properties of Th(IV) on the raw diatomite: effects of contact time, pH, ionic strength and temperature. *Appl Radiat Isot*, 2008, 66: 1313–1320
23 Qian LJ, Zhao JN, Hu PZ, Geng YX, Wu WS. Effect of pH, fulvic acid and temperature on sorption of Th(IV) on zirconium oxophosphate. *J Radioanal Nucl Chem*, 2010, 283: 653–660
24 Wang MM, Tao XQ, Song XP. Effect of pH, ionic strength and temperature on sorption characteristics of Th (IV) on oxidized multiwalled carbon nanotubes. *J Radioanal Nucl Chem*, 2011, 288: 859–865
25 Li P, Fan QH, Pan DQ, Liu SP, Wu WS. Effects of pH, ionic strength, temperature, and humic acid on Eu(III) sorption onto iron oxides. *J Radioanal Nucl Chem*, 2011, 289: 757–764
26 Chen SW, Guo BL, Wang YL, Li Y, Song LJ. Study on sorption of U(VI) onto ordered mesoporous silicas. *J Radioanal Nucl Chem*, 2013, 295: 1435–1442
27 Tan XL, Wang XK, Fang M, Chen CL. Sorption and desorption of Th(IV) on nanoparticles of anatase studied by batch and spectroscopy methods. *Colloid Surface A*, 2007, 296: 109–116
28 Langmuir I. The adsorption of gases on plane surfaces of glass, mica and platinum. *J Am Chem Soc*, 1918, 40: 1361–1403
29 Freundlich HMF. Over the adsorption in solution. *J Phys Chem*, 1906, 57: 1100–1107
30 Dubinin M. The potential theory of adsorption of gases and vapors for adsorbents with energetically nonuniform surfaces. *Chem Rev*, 1960, 60: 235–241
31 Özcan AE, Öncü EM, Özcan AS. Kinetics, isotherm and thermodynamic studies of adsorption of Acid Blue 193 from aqueous solutions onto natural sepiolite. *Colloid Surface A*, 2006, 277: 90–97
32 Lin SH, Wang CS. Treatment of high-strength phenolic wastewater by a new two-step method. *J Hazard Mater*, 2002, 90: 205–216
33 Chen L, Gao X. Thermodynamic study of Th(IV) sorption on attapulgite. *Appl Radiat Isot*, 2009, 67: 1–6
34 Fan QH, Wu WS, Song XP, Xu JZ, Hu J, Niu ZW. Effect of humic acid, fulvic acid, pH and temperature on the sorption-desorption of Th(IV) on attapulgite. *Radiochim Acta*, 2008, 96: 159–165
35 Yu SM, Ren AP, Chen CL, Chen YX, Wang X. Effect of pH, ionic strength and fulvic acid on the sorption and desorption of cobalt to bentonite. *Appl Radiat Isot*, 2006, 64: 455–461
36 Xu D, Zhou X, Wang XK. Adsorption and desorption of $Ni^{2+}$ on Na-montmorillonite: effect of pH, ionic strength, fulvic acid, humic acid and addition sequences. *Appl Clay Sci*, 2008, 39: 133–141